07 - 10 September 2009

PROCEEDINGS

54. IWK

Internationales Wissenschaftliches Kolloquium
International Scientific Colloquium

Information Technology and Electrical Engineering - Devices and Systems, Materials and Technologies for the Future

Faculty of Electrical Engineering and Information Technology

Startseite / Index:
http://www.db-thueringen.de/servlets/DocumentServlet?id=14089

TECHNISCHE UNIVERSITÄT
ILMENAU

Impressum

Herausgeber: Der Rektor der Technischen Universität Ilmenau
Univ.-Prof. Dr. rer. nat. habil. Dr. h. c. Prof. h. c.
Peter Scharff

Redaktion: Referat Marketing
Andrea Schneider

Fakultät für Elektrotechnik und Informationstechnik
Univ.-Prof. Dr.-Ing. Frank Berger

Redaktionsschluss: 17. August 2009

Technische Realisierung (USB-Flash-Ausgabe):
Institut für Medientechnik an der TU Ilmenau
Dipl.-Ing. Christian Weigel
Dipl.-Ing. Helge Drumm

Technische Realisierung (Online-Ausgabe):
Universitätsbibliothek Ilmenau
ilmedia
Postfach 10 05 65
98684 Ilmenau

Verlag:
Verlag ISLE, Betriebsstätte des ISLE e.V.
Werner-von-Siemens-Str. 16
98693 Ilmenau

ISBN (USB-Flash-Ausgabe): 978-3-938843-45-1
ISBN (Druckausgabe der Kurzfassungen): 978-3-938843-44-4

Startseite / Index:
http://www.db-thueringen.de/servlets/DocumentServlet?id=14089

PARASITIC EFFECTS ON ELECTRICAL MACHINES: ESTIMATION AND MINIMIZATION CONSIDERING NON-IDEAL MANUFACTURING

Mercedes Herranz Gracia / Isabel Coenen / Kay Hameyer

Institute of Electrical Machines
RWTH Aachen University
Schinkelstrasse 4, 52056 Aachen, Germany

ABSTRACT

Electrical machines used as servo-drive are more efficient and offer a better dynamic behavior when compared to hydraulic or pneumatic drives. However, they present parasitic effects, such as cogging torque or acoustic noise, which disturb their function and therefore need to be minimized. The manufacturing process and the fabrication tolerances of the motor components have a strong influence on the mentioned parasitic effects. Therefore, such influences on the electrical machine must be considered to estimate and minimize the unwanted effects. This paper presents an overview on the estimation and minimization of the cogging torque of a permanent-magnet synchronous machine (PMSM) and the acoustic noise of an induction motor (IM) used as servo-drive.

Index Terms— Electrical machines, cogging torque, noise, tolerances

1. INTRODUCTION

The use of electrical drives on industry and automotion is on constant expansion due to their advantages on efficiency and dynamic compared to other drive alternatives.

The working principle of electrical drives produces some undesirable parasitic effects, such as torque ripple, electromagnetic noise and magnetic losses. Therefore, the optimization of electrical drives implies necessarily the minimization of the parasitic effects. This minimization is usually done ignoring the influence of non-ideal manufacturing.

It has been shown that the variations from the ideal machine due to geometric and material tolerances have a strong effect on the parasitic effects and specially on the cogging torque and the electromagnetic noise [1][2]. The neglection of this fact on the minimization of the parasitic effects results on an optimum, which is not robust against manufacturing faults.

This paper presents an overview on the problematic of cogging torque and acoustic noise considering non-ideal manufacturing conditions. First, the estimation methods for both parasitic effects are presented. The most critical manufacturing faults are then discussed and an example of practical minimization of each parasitic effect is presented.

2. COGGING TORQUE

On PMSMs, cogging torque is already caused under no-load condition by the interaction between the rotor magnets and the stator slots. This results in unwanted effects such as vibrations and deformations. Especially in application as a servo-drive, this is a very critical issue. Hence, a minimization of cogging torque is required.

2.1. Origins and estimation

Due to the stator slotting of the estimated machine, the air gap width and therefore the magnetic permeance at the air gap alternates periodically. Because of the thereby evoked oscillating magnetic energy and the rotor's inclination to positions with maximum stored energy, a pulsating torque is generated.

In this study, the computation of the cogging torque is performed by the Finite Element Method (FEM). The studied machine is simulated under no-load condition and the torque T is computed with Maxwell Stress Tensor along a cylindrical surface around the rotor:

$$T = \frac{l_z}{\mu_0} \int_\Gamma r \cdot B_r \cdot B_t \cdot d\Gamma. \tag{1}$$

At this, Γ is a closed contour around the rotor at radius r, l_z is the length of the machine and B_r and B_t are the radial and tangential component of the magnetic flux density.

2.2. Influence of non-ideal manufacturing

Two tolerances of non-ideal manufacturing are considered within this study, which influence on cogging torque is known as critical. These are variance of the magnet's remanence flux-density and static eccentricity of the rotor.

2.2.1. Variance of remanence flux-density

The occurrence of magnetization faults results in an asymmetrical distribution of the air gap flux-density which implicates additional content of cogging torque [1]. Within this study, a variance at the magnet's remanence flux density B_R by $\pm 5\%$ is considered. For the estimated machine with its eight permanent magnets at the rotor, 18 independent configurations can be evaluated as relevant [3].

Figure 1 shows the cogging torque, related to its reference value, for the 18 configurations where a variance at B_R by -5% is considered. One octagon represents the eight magnets of the machine and a circle marks a magnet which remanence flux-density varies. It shows that every configuration results in a higher cogging torque than the reference without magnetization faults. But there is a difference in the influence on cogging torque for the particular configurations.

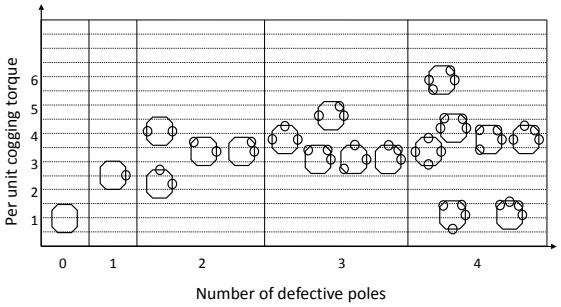

Fig. 1. Cogging torque distribution for the 18 configurations.

2.2.2. Static eccentricity

In case of a static eccentricity, the rotor center is displaced into a fixed eccentric position. This results in higher contents of cogging torque due to the asymmetrical behavior of the flux-density at the air gap. Figure 2 shows the cogging torque distribution for the 18 configurations with static eccentricity compared to the distribution from figure 1. The distributions show similarities, whereas the one with eccentricity shows higher cogging torque values.

2.3. Minimization

To achieve the cogging torque minimization the machine's geometry is optimized. The influence of various design parameters is estimated by using Design of Experiments [4] in combination with FE simulations. By conducting a series of factorial design, the width of the magnet b_M and the width of the slot opening b_S appear to be significant parameters concerning the cogging torque for the estimated machine.

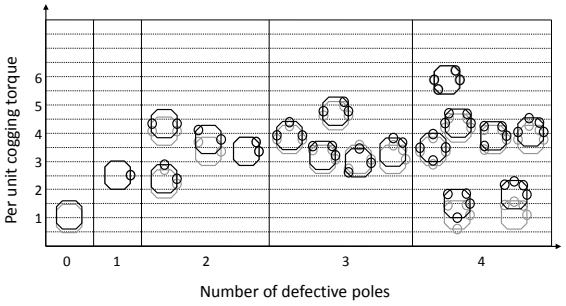

Fig. 2. Cogging torque distribution for the 18 configurations with static eccentricity.

The optimization is performed with respect to the above manufacturing tolerances, aiming at a minimized cogging torque characteristic, which is robust against such tolerances. As a first step, the 18 relevant configurations are minimized separately. For each of them, a 2^2-factorial design is applied with b_M and b_S as factors which are varied in two levels. Table 1 shows the matrix of this design with the peak-to-peak cogging torque ΔT as output value of each of the four experiments. From the results the coefficients of a polynomial can be determined:

$$\hat{y} = c_0 + c_1 x_1 + c_2 x_2 + c_{12} x_1 x_2. \qquad (2)$$

This polynomial is analyzed with the method of gradient descent to determine a minimum for the two design parameters.

Table 1. 2^2-factorial design.

Experiments			Independent variables				Output
	b_M	b_S	0	1	2	12	
1	-	-	+	-	-	+	ΔT_1
2	+	-	+	+	-	-	ΔT_2
3	-	+	+	-	+	-	ΔT_3
4	+	+	+	+	+	+	ΔT_4
Coefficients			c_0	c_1	c_2	c_{12}	

Finally, an overall design optimum for the machine, which includes every configuration and therefore the non-ideal manufacturing, can be determined by a statistical evaluation. Thereby, the worst case where half of the permanent magnets are defective is considered and the probability of occurrence for the particular configurations is determined. At last, a weighted average value for b_M and b_S can be calculated, representing the design optimum.

To verify the results of the minimization, a stochastic numerical analysis is performed. At this, the remanence flux-density is considered to be normally dis-

tributed [5]. Figure 3 shows the density function

$$f(x) = \frac{1}{\sigma\sqrt{2\pi}} \cdot \exp(-\frac{1}{2}(\frac{x-\mu}{\sigma})^2) \qquad (3)$$

of the normal distribution. In this study, the remanence flux-density is regarded as variable x with the expected value μ and a tolerance width Δx of 5% which is equal to the triple standard deviation $\sigma = \frac{\Delta x}{3}$.

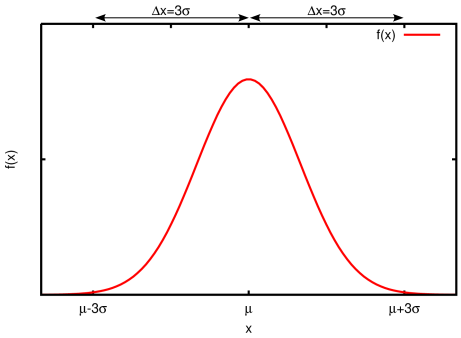

Fig. 3. Density function of the normal distribution.

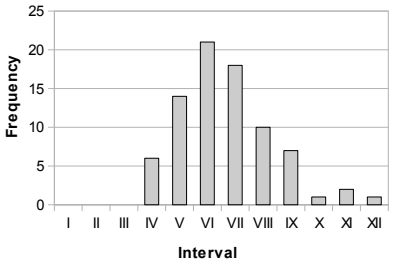

(a) Reference geometry.

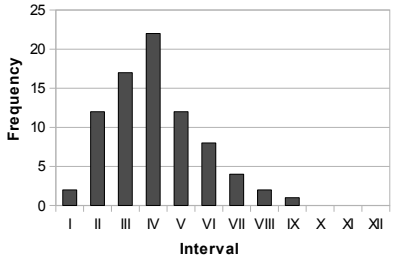

(b) Optimized geometry.

Fig. 4. Frequency distribution.

By use of the Box-Muller method [6] normally distributed random values z_i are generated and transformed into variables $x_i = \mu + z_i \cdot \sigma$ of the normal distribution. Finally, for each magnet a random value of its remanence flux-density is generated in such a way that a series of 80 random configurations is created. The cogging torque is simulated for each of these configurations, with original geometry of the machine as well as with optimized geometry. The results are divided into twelve intervals, where interval I represents the lowest cogging torque values and interval XII the highest values. Figure 4 illustrates the resulting frequency distribution for both geometries. It shows the reduction of cogging torque which is achieved by applying the optimized geometry.

3. ACOUSTIC NOISE

Noise from electrical machines is gaining impact due to the rising demands on job-safety and user comfort. Acoustic noise from servo-drives has electromagnetic as well as aerodynamic and mechanical origins. However, electromagnetic noise is generated as single tones on frequencies, where the human ear is specially sensitive and, therefore, it is main responsible for noise on electrical machines.

3.1. Origins

Noise perception results from the combination of three elements: a vibrating body, a medium, which transports the vibration and a hearer sensing a noise due to the vibration. On electrical machines, the air-gap flux density originates radial forces on the stator teeth. This forces produce a vibration on the stator i.e. on its yoke and this vibration is transmitted as airborne or structure-borne noise till the hearer.

The radial surface force acting on the stator teeth σ can be calculated with the simplified Maxwell Stress Tensor by:

$$\sigma_r(x,t) = \frac{B^2_{\delta,r}(x,t)}{2\mu_0}, \qquad (4)$$

where $B_{\delta,r}$ is the radial flux density in the air-gap.

Given two flux density waves $B_a(x,t)$ and $B_b(x,t)$,

$$B_a(x,t) = B_a\cos((\nu_a x - \omega_{\nu_a})t - \phi_{a)} \qquad (5)$$

$$B_b(x,t) = B_b\cos((\nu_b x - \omega_{\nu_b})t - \phi_{b)} \qquad (6)$$

the radial force generated by them is

$$\begin{aligned}\sigma_{a,b}(x,t) = \tfrac{1}{2\mu_0}(\tfrac{B_a^2}{2}(1+\cos(2\nu_a x - 2\omega_{\nu_a}t - 2\phi_a)) \\ +\tfrac{B_b^2}{2}(1+\cos(2\nu_b x - 2\omega_{\nu_b}t - 2\phi_b)) \\ +B_a^2 \cdot B_b^2\cos((\nu_a \pm \nu_b)x - (\omega_{\nu_a} \pm \omega_{\nu_b})t - (\phi_a \pm \phi_b)).\end{aligned} \qquad (7)$$

The mode-number r of a surface-force wave represents the number of spatial maxima of it and can be calculated from the pole pair numbers of the flux-density waves, which interact to originate the surface-force:

$$r_{ab} = \nu_a \pm \nu_b. \qquad (8)$$

Fig. 5 shows surface-force waves with mode-numbers smaller than six.

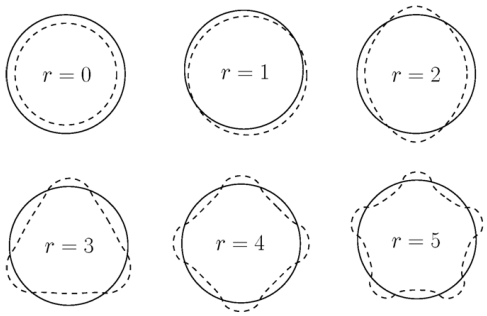

Fig. 5. Mode-number r of a radial surface-force wave.

Similarly, the angular speed of the surface force can be calculated as follows:

$$\omega_{ab} = \omega_{\nu_a} \pm \omega_{\nu_b}. \tag{9}$$

The deformation of the stator yoke decreases proportionally with the mode-order of the force excitation. Mode-orders smaller than six are critical. Equations (8) and (9) can therefore be used to identify the critical frequency-orders of the acoustic noise and trace back their origin in terms of air-gap flux-density components.

3.2. Estimation methods

Noise in electrical machines is a complex problem due to its multiphysical nature (Electromagnetism, Mechanics and Acoustics). Both, analytical and numerical methods are proposed in the literature [7].

Analytical methods allow systematically studying the entire chain of effects leading to the generation of noise, from the stator currents to the deformation. Therefore, they are very useful for the identification of cause-and-effect relationships but not for their quantification due to its limitations on the description of the steel nonlinearity and the resonance frequencies of the structure.

On the other hand, numerical methods i.e. coupled electromagnetic-mechanical FEM simulations are much more accurate, although also computationally more expensive and unable to prove a causal link between a specific flux-density component and noise.

Therefore, the most efficient approach consists of a combination of analytical and numerical methods is presented in this paper. The analytical model is used to identify cause-and-effects relationships. A coupled FE simulation allows afterward the quantification of this relationships.

3.2.1. Analytical model

The identification of the critical frequency-orders and mode-orders and its origins is done using order tables [8]. They allow a simple and effective representation of the combination of stator harmonics, which are represented on the columns of the table, and rotor harmonics, which can be found on the rows of the table, and how this combination leads to forces with the corresponding mode and frequency-order.

Table 2 shows the order table for an induction machine (IM) with $p = 2$ pole pairs and $N_2 = 26$ rotor slots. It can be read that the stator harmonic with pole-pair number $\nu_1 = 26$ and the rotor harmonic with pole-pair number $\nu_2 = -24$ results on a radial force wave with the critical mode-number $r = 2$ and a frequency $f = 21 \cdot f_m$.

Table 2. Order table for an IM with $p = 2$ and $N_2 = 26$. Only $r \leq |8|$ are indicated.

			Stator harmonics					
		ν_1	2	-10	14	-22	26	$\frac{\omega_r}{\omega_m}$
	ν_2							
Rotor harmonics	2	+	4	-8				5.0
		-	0					0.0
	-24	+					2	-21.0
		-				2		26.0
	28	+				6		31.0
		-					-2	-26.0

3.2.2. Numerical model

For the numerical study of the structural-dynamic behavior of the machine, a 2D transient electromagnetic simulation is first performed. The electromagnetic surface-force densities are extracted from the solution with the Maxwell Stress Tensor and transformed into the frequency domain. They are then used as excitation for the structural-dynamic simulation. The resulting deformation can be used as input for an acoustic simulation or it can be integrated to calculate the body-sound index. The body-sound index for a specific frequency $L(f)$ is an integral value related to the deformation of a body, in this case the stator. It is defined as the sum of the square of the normal component of the velocity of deformation $|\vec{v} \cdot \vec{n}|$ for all the finite elements p in the surface S of the body [9],[10]:

$$L(f) = 10\log\left(\frac{\sum_p \int_{S_p} |\vec{v_p} \cdot \vec{n^p}|^2 \mathrm{d}S}{S_0 \cdot h_{U_0}^2}\right) \tag{10}$$

$S_0 = 1\mathrm{m}^2$ and $h_{U_0}^2 = 250 \cdot 10^{-15}\mathrm{m}^2$ are reference values.

Fig 6 shows an overview of the numerical simulation procedure.

If the axial behavior of the structure is to be analyzed, for example in the case that the machine is only fixed at one axial end of the machine, a three dimensional structure-dynamic simulation, which is computationally very expensive, is necessary. For differential

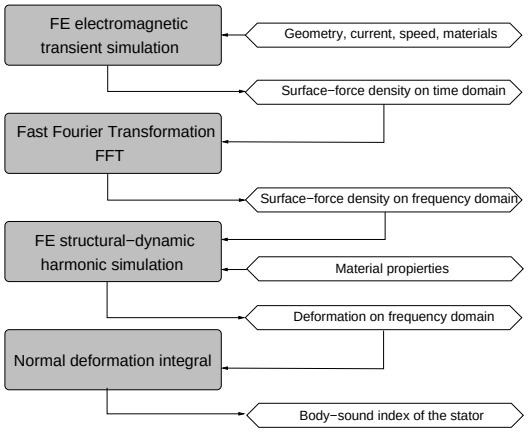

Fig. 6. Overview of the numerical simulation procedure.

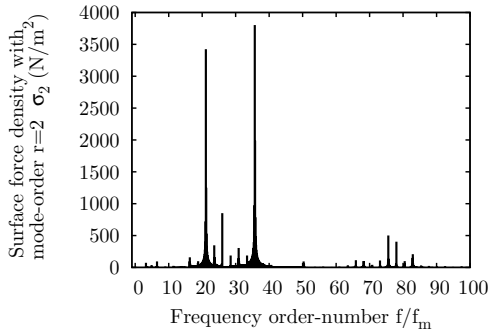

Fig. 7. Surface force-density with mode-number $r = 2$ for an IM with $p = 2$ and $N_2 = 26$.

analysis between two geometry variants, the comparison of the electromagnetic force excitation is enough. This reduces drastically the computational effort because the force can be extracted directly from the electromagnetic simulation.

Fig 7 shows the surface-force density with mode-number $r = 2$ (ovalization mode) for the also analytically studied IM on the frequency domain. Thanks to the numerical analysis, it is possible to quantify the force density with mode-number $r = 2$ and frequency $f = 21 \cdot f_m$, whose origin has been already identified with Table 2.

The deformations on the machine due to this excitation forces may be calculated in two different ways. The first possibility is a modal analysis of the structure. The transfer function of the structure extracted from the modal analysis can be then used for a wide-band computation of the deformation. An alternative approach is an harmonic mechanical simulation of the relevant frequency using the forces from the electromagnetic simulation as excitation. Because electric drives produce only forces with single frequencies, which are easily identifiable by order-tables (see Table 2) this method is preferred.

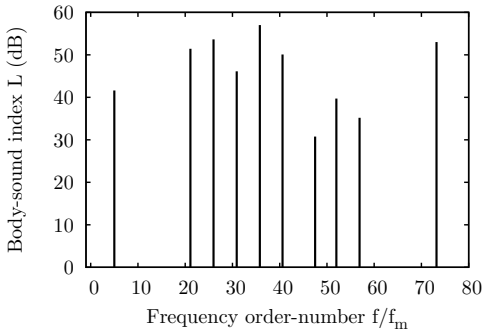

Fig. 8. Body-sound index of the stator of an IM with $p = 2$ and $N_2 = 26$.

Fig 8 shows the body-sound index L computed by (10) for the studied IM. The deformation with the frequency-order 21 is due to the ovalization form of the exciting force critical, confirming the analytical results.

3.3. Influence of a non-ideal manufacturing conditions

The manufacturing process of an electrical drive produces due to geometrical tolerances or material inhomogeneities variations from the ideal conditions. These deviations such as eccentricity, cutting notches, magnetic anisotropy, current harmonics or permanent-magnet tolerances have a negative influence on the acoustic behavior of the machine because they generate new force excitations. Due to its capital importance [11], [12] , the effect of the eccentricity on the acoustic behavior is discussed as example.

3.3.1. Eccentricity

Eccentricity occurs if the stator and the rotor of the machine does not have the same center and it results on a non-uniform air-gap. Due to the geometrical tolerances, all electrical machines are up to some extend eccentric.

The non-uniformity of the air-gap caused by the eccentricity can be described as an air-gap magnetic permeance wave with the pole-pair number $\nu_\epsilon = 1$. From its combination with stator and rotor harmonics, new surface-force waves result. The mode-order number of this new waves r_ϵ can be calculated from the mode-order number of the surface-force waves of the machine without eccentricity $r_{original}$ as

$$r_\epsilon = r_{original} \pm \nu_\epsilon = r_{original} \pm 1 \qquad (11)$$

Therefore, the surface-force waves of the centric machine with the uncritical mode-order $r = 0$ results under eccentricity conditions on surface-force waves with mode-order $r = 1$ i.e. on oscillating global forces.

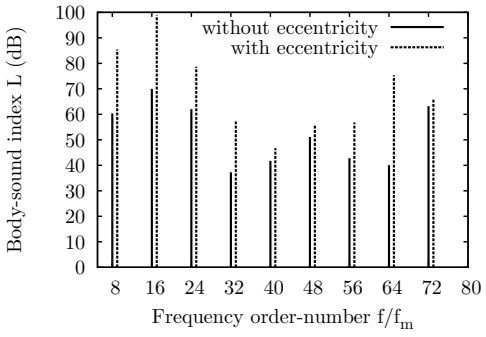

Fig. 9. Body-sound index of the stator of a PMSM with and without static eccentricity.

The machine reacts strongly to this kind of forces and, therefore, large deformations occur.

This critical effect of the eccentricity on the acoustic behavior of the machine can be observed in Fig. 9. It shows the body-sound index of the stator of a PMSM with and without static eccentricity. An increase of up to 20 dB occurs due to this manufacturing fault.

3.4. Example of noise reduction

As seen previously, the evaluation of the electromagnetic, structural and acoustic behavior of an electrical drive is computationally expensive. Direct optimization algorithms are therefore not applicable. An alternative approach is the methodology of Design of Experiments and Response Surface as it has been used on section 2.

3.4.1. Objectives

The already presented IM is optimized using this method. The outer dimensions of the machine (stator outer radius, shaft radius, etc.) and the main configuration of the machine (number of pole pairs, number of stator and rotor slots, etc.) are given. Hence they are not considered as optimization parameters.

The objective of the optimization is the minimization of the vibration given by the electrical machine to the mechanical load. The induction machine transmits vibration in two different ways. First, the torque ripple is delivered through the shaft into the mechanical load. On the other hand, the electromagnetic forces acting on the stator of the machine produce a vibration, which is transmitted via the housing to the mechanical load. Moreover, the delivery of the rated torque must be ensured.

3.4.2. Model evaluation

The delivered torque (T) and torque ripple (ΔT) can be evaluated easily through a 2D finite element electromagnetic simulation. The evaluation of the vibration transmitted via the stator and the housing require a coupled simulation. Neglecting the axial deformation with a 2D structure dynamical simulation, a fast evaluation, one minute per frequency, of the deformation of the machine is possible [13]. To reduce the computational effort further, only frequencies with a significant force excitation are considered. This results in eleven structure dynamical simulations for each model evaluation.

For the employment in the optimization, the structure-dynamic behavior for the different frequencies is summarized as the logarithmic sum of the body-sound index for all significant frequencies (L).

The evaluation of these three objectives (minimization of L and ΔT and maintenance of T) with the coupling of the transient electromagnetic 2D simulation and the harmonic structure-dynamic 2D simulation takes about 3 hours.

3.4.3. Optimization parameters

The choice of the parameters or factors of the optimization is one of the critical points of the process. As a preliminary step of the optimization a sensibility analysis was performed for a set of eight parameters. This analysis was conducted using simple analytical and electromagnetic numerical models and took about the same amount of time as the optimization itself. Only three of the studied parameters have shown a significant influence on the response variables. The first one is the air-gap length (A). The other two are related with the mechanical connection between stator and housing. This connection is ensured through six clamping bolts. Both stator and housing have six notches to keep these clamping bolts. Both the depth of this mounting notches in the outer contour of the stator (D) and its position (P) are taken as optimization parameters.

3.4.4. Optimization procedure and results

A full factorial design-of-experiment is used to sample the parameter space. The response surface for the three response variable is build using first (for D and P) and second order polynomial (for A). The optimization is then performed on these response surfaces taking into account the mechanical constraints and using the method of gradient descent.

Table 3 shows the values of the geometry parameters before and after the optimization. The results of the optimization are shown in Fig. 10. The torque ripple and the logarithmic sum of the body-sound index have been reduced respectively in 30% and 4.6 dB, which implies a diminution of about 50% in the deformation of the stator. The delivered torque after the optimization is 6% higher as the rated one. This is due to the linear approximation of the torque behavior and can be easily counteracted with a smaller current in the motor.

Table 3. Value of the parameter before and after the optimization.

Parameter	Reference	Optimum
A	0.2 mm	0.25 mm
D	3.5 mm	2.1 mm
P	notch over a slot	notch over a tooth

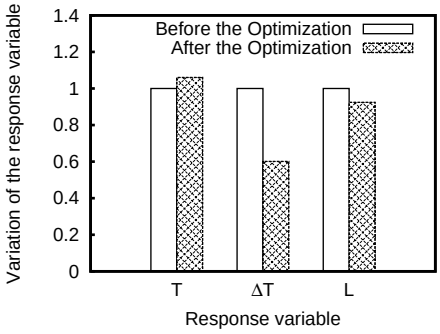

Fig. 10. Response variable before and after the optimization.

4. CONCLUSIONS

This paper shows an overview of the estimation and minimization methods of two parasitic effects from electrical drives: cogging torque and acoustic noise.

The influence of non-ideal manufacturing on the optimization has been illustrated with the minimization of the cogging torque of a PMSM, considering eccentricity and tolerances of the remanence of permanent magnet. The use of numerical simulations combined with statistical Design of Experiments results in a robust design of the machine, which is validated by stochastic FEM.

The same procedure is also successful on the minimization of the acoustic noise produced by an IM in spite of the multiphysical nature of the problem.

5. REFERENCES

[1] Lovrenc Gašparin, Andrej Cernigoj, Stojan Markic, and Rastko Fišer, "Prediction of cogging torque level in PM motors due to assembly tolerances in mass," *COMPEL: The International Journal for Computation and Mathematics in Electrical and Electronic Engineering*, vol. 27, pp. 911 – 918, 2008.

[2] C. Schlensok and K. Hameyer, "Body-Sound Analysis of a Power-Steering Drive Considering Manufacturing Faults," *IEEE Transactions on Vehicular Technology*, vol. 56, no. 4, pp. 1553–1560, July 2007.

[3] C. Schlensok, M. Kurzidem, and K. Hameyer, "Novel method for fast analysis of cogging-torque harmonics in permanent-magnet synchronous-machines," in *12th Biennial IEEE Conference on Electromagnetic Field Computation, CEFC 2006*, Miami, USA, May 2006, pp. 330–330.

[4] D. C. Montgomery, "Design and analysis of experiments," *John Wiley & Sons*, New York 1976.

[5] S.-B. Yoon, I.-S. Jung, and D.-S. Hyun, "Robust shape optimization of electromechanical devices," *IEEE Transactions on Magnetics*, vol. 35, pp. 1710–1713, May 1999.

[6] G. E. P. Box and M. E. Muller, "A note on the generation of random normal deviates," *Annals of Mathematical Statistics*, vol. 29, pp. 610–611, 1958.

[7] Jacek F. Gieras, Chong Wang, and Joseph Cho Lai, *Noise of Polyphase Electric Motors*, Marcel Dekker Inc, Dec. 2005.

[8] Hans Otto Seinsch, *Oberfelderscheinungen in Drehfeldmaschinen*, B. G. Teubner, Stuttgart, 1992.

[9] C. Schlensok, D. van Riesen, T. Küest, and G. Henneberger, "Acoustic Simulation of an Induction Machine with Squirrel-Cage Rotor," *COMPEL*, vol. 25, no. 2, pp. 475–486, 2006.

[10] F. G. Kollmann, *Maschinenakustik: Grundlagen, Messtechnik, Berechnung, Beeinflussung*, Springer Verlag, Berlin, Heidelberg, New York, Barcelona, Budapest, Hong Kong, London, Mailand, Paris, Santa Clara, Singapore, Tokyo, 2000.

[11] M.J. DeBortoli, S.J. Salon, D.W. Burow, and C.J. Slavik, "Effects of rotor eccentricity and parallel windings on induction machine behavior: a study using finite element analysis," *IEEE Transactions on Magnetics*, vol. 29, no. 2, pp. 1676–1682, Mar. 1993.

[12] Christoph Schlensok and Gerhard Henneberger, "Calculation of force excitations in induction machines with centric and excentric positioned rotor using 2D Transient FEM," in *14th Conference on Computation of Electromagnetic Fields*, Saratoga Springs, USA, July 2003, COMPUMAG.

[13] M. van der Giet, C. Schlensok, B. Schmülling, and K. Hameyer, "Comparison of 2-D and 3-D Coupled Electromagnetic and Structure-Dynamic Simulation of Electrical Machines," *IEEE Transactions on Magnetics*, vol. 44, no. 6, pp. 1594–1597, June 2008.